Loading silica with metals (palladium or platinum) under mild conditions by using well-defined molecular precursors†

Lidia Armelao,*[a] Daniela Belli Dell'Amico,*[b] Roberto Braglia,[c] Fausto Calderazzo,[b] Fabio Garbassi,[c] Gianluigi Marra[c] and Alessandra Merigo‡[b]

Received 23rd February 2009, Accepted 18th May 2009
First published as an Advance Article on the web 8th June 2009
DOI: 10.1039/b903655e

The loading of pre-treated amorphous silica with platinum or palladium was carried out by using the molecular precursors $Pt_2(\mu\text{-}Cl)_2Cl_2(CO)_2$, or $Pd_2(\mu\text{-}Cl)_2Cl_2(CO)_2$, respectively, which contain the required amount of coordinated CO to carry out the formation of the metal particles upon contact with moisture. The reactivity of the well-soluble mononuclear platinum complex *cis*-$PtCl_2(CO)_2$ with stoichiometric amounts of water was investigated either under N_2 or CO. The metal nanoparticles produced on the silica matrix have been characterized by X-ray photoelectron spectroscopy (XPS), X-ray diffraction (XRD) and transmission electron microscopy (TEM). The catalytic performance of the silica-supported metals thus produced was evaluated in the hydrogenation of cyclohexene.

Introduction

The formation of metal nanoparticles is an expanding area of research,[1] in connection with: (a), the use of well-defined molecular precursors; (b), the understanding of the aggregation phenomena; (c) the application to several areas of surface science. When the precursor contains a metal characterized by a positive standard reducing potential, its prompt reduction (by heat or by exposure to H_2, or to CO/H_2O) is to be expected, with formation of metal nanoparticles, whose dimensions depend, among other factors, on the temperature. In this regard, the observation[2] was made that a higher catalytic activity in the hydrogenation of several substrates was found for catalysts obtained under milder reducing conditions. The preparation of supported noble metal nanoparticles and the study of their efficiency in hydrogenation catalysis is a topic of current interest.[3]

In earlier reports from these laboratories, palladium, platinum and gold have been supported on silica by using the corresponding *N,N*-dialkylcarbamato complexes as precursors.[4] Also the mononuclear chlorocarbonyls AuCl(CO) and *cis*-$PtCl_2(CO)_2$ were used for the same purpose.[4c,5] This paper presents the results obtained with $Pt_2(\mu\text{-}Cl)_2Cl_2(CO)_2$ and $Pd_2(\mu\text{-}Cl)_2Cl_2(CO)_2$.[6,7] As the precursors are similar from a molecular viewpoint (both are chloride-bridging species),[6b] the Pd/Pt comparison was anticipated to be particularly interesting. These dinuclear derivatives were expected to bind to the oxygen atoms on the silica surface by splitting of the chloride bridges, with subsequent attack by water thus reducing the platinum(II) and palladium(II) centres, CO being converted to CO_2. The presence in the dinuclear precursors of only one CO group *per* metal atom and, consequently, of two reducing equivalents, was considered to be ideal for converting the central metal atom to the zerovalent state, *i.e.* to $M_{(s)}$. A further advantage in the use of the chloro-carbonyl derivatives of palladium and platinum is that their reaction with moisture occurs at room temperature or even lower. This feature was anticipated to limit aggregation of the resulting metal particles, normally favoured at higher temperatures.

Interest in this study also comes from comparing chemical properties within metals characterized by a decreasing metal–metal bond strength, as evaluated on the basis of the corresponding enthalpies of formation of gaseous atoms (kJ mol^{-1}): Pt, 565.7; Pd, 376.6.[8] As a test of the Pd/Pt comparison we decided to investigate the catalytic performance of the platinum-loaded silica with the corresponding palladium-containing system. A final remark concerns the use of amorphous silica of a relatively high surface area as a support.

Results and discussion

Reaction of the molecular precursors with water

As explained in the Introduction, this study deals with loading the silica surface with platinum and palladium by using the dinuclear $M_2(\mu\text{-}Cl)_2Cl_2(CO)_2$ (M = Pd, Pt), which are planar chloride-bridged species.[6b]

Taking into consideration that even dehydrated silica, see *Experimental*, can be a source of water through condensation of the surface silanol groups, it was of interest to know the outcome of the reaction of the chlorocarbonyl derivatives of these metals with *a stoichiometric, or slightly higher*, amount of water. Concerning the palladium derivative, we had previously noted[7b] that $Pd_2(\mu\text{-}Cl)_2Cl_2(CO)_2$ is reduced by CO in acetic anhydride with formation of $[PdCl(CO)]_n$ and later we have verified[9] that the same product results when the $PdCl_2/CO$ system is contacted with water (H_2O/Pd molar ratios in the range 1–3). Recently, the assistance

---

[a] *ISTM-CNR and INSTM–Dipartimento di Scienze Chimiche–Università di Padova–Via Marzolo, 1–35131, Padova, Italy. E-mail: lidia.armelao@unipd.it*
[b] *Dipartimento di Chimica e Chimica Industriale, Università di Pisa, Via Risorgimento 35, I-56126, Pisa, Italy. E-mail: belli@dcci.unipi.it*
[c] *Istituto ENI Donegani, Via G. Fauser 4, I-28100, Novara, Italy*

† This paper is dedicated to the memory of the late Prof. Carlo Carlini, Università di Pisa.

‡ Present address: *Lucchini L. R. S., Viale della Resistenza 2, I-57025 Piombino, Livorno, Italy*

of water in the formation of $[PdCl(CO)]_n$ from $PdCl_2$ under CO has been reported by another group.[10]

The reduction of *cis*-$PtCl_2(CO)_2$ in the presence of an excess of water has been reported by Chatt and co-workers,[11] the reaction being carried out *under carbon monoxide* in ethanol as medium. In the present study, the reaction of *cis*-$PtCl_2(CO)_2$ [preferred to $Pt_2(\mu\text{-}Cl)_2Cl_2(CO)_2$ in view of its higher solubility in hydrocarbons] with 1, 2 and 3 equivalents of water was carried out both under N_2 and under CO. Ethanol was excluded as solvent because of its possible interference in the reduction process.

Under an atmosphere of pre-purified dinitrogen and at room temperature, a toluene solution of the mononuclear carbonyl derivative of platinum(II) undergoes reduction in the presence of dissolved water, ligated carbon monoxide being partially converted to carbon dioxide, see eqn (1). Disappearance of the typical carbonyl bands of *cis*-$PtCl_2(CO)_2$ was observed at a H_2O/Pt molar ratio of 3, a black solid analysing as $[PtCl(CO)]_n$ (60% yield) being obtained (ν_{CO}, 2060 cm^{-1}) which was recovered by filtration.

$$2\ cis\text{-}PtCl_2(CO)_2 + H_2O \rightarrow 2/n[PtCl(CO)]_n + 2\ HCl + CO_2 + CO \quad (1)$$

The platinum-containing product of reaction (1), after drying *in vacuo*, was identified through its reaction with $[NBu_4]Cl$ in CH_2Cl_2 yielding the already known[12] compound $[NBu_4]_2[Pt_2Cl_4(CO)_2]$ in good yields (≥70%), see eqn (2).

$$2/n[PtCl(CO)]_n + 2[NBu_4]Cl \rightarrow [NBu_4]_2[Pt_2Cl_4(CO)_2] \quad (2)$$

The formation of platinum(I) under the conditions of reaction (1) was therefore established. As $[PtCl(CO)]_n$ is substantially insoluble in the reaction medium, its further reduction to platinum(0) presumably becomes unfavourable. Furthermore, the HCl produced in the reaction interacts with H_2O, thus reducing its activity in solution, and an excess of water is consequently required to perform reaction (1).

Under CO at room temperature, the reaction between *cis*-$PtCl_2(CO)_2$ and water goes to completion with a H_2O/Pt molar ratio of 2.5 leading to the formation of the violet-black $[Pt(CO)_2]_n$[11] (≥97% yield). The CO-promoted reduction of platinum(II) can therefore be represented by reaction (3).

$$cis\text{-}PtCl_2(CO)_2 + H_2O + CO \rightarrow 1/n[Pt(CO)_2]_n + 2HCl + CO_2 \quad (3)$$

In separate experiments we observed that $[PtCl(CO)]_n$ reacts in toluene with excess water: (a) under N_2 with production of a solid containing 95% of platinum; (b) under CO with formation of $[Pt(CO)_2]_n$.

It is noteworthy that $[Pt(CO)_2]_n$ is not stable and irreversibly loses CO (*in vacuo* or by thermal treatment) to finally yield platinum metal.[13]

Loading of silica

When dehydrated silica was treated under a dinitrogen atmosphere with a solution of the orange $Pt_2(\mu\text{-}Cl)_2Cl_2(CO)_2$ at room temperature, the platinum-containing fragments migrate from solution to the SiO_2 surface, as evidenced by the colour of the silica turning to orange. We propose adsorption of platinum(II) to be the primary process, followed by grafting as a consequence of chloride-bridge splitting and formation of $PtCl_2(CO)$ fragments bonded to the oxygen atoms of the silica surface. The platinum-grafted silica, after being recovered by filtration, was subjected to a treatment with water vapour at 40 °C in order to carry out the exhaustive reduction to zerovalent platinum, as for eqn (4).

$$Pt_2Cl_4(CO)_2 + 2H_2O \rightarrow 2CO_2 + 4HCl + 2Pt_{(s)} \quad (4)$$

The platinum-loaded silica samples, before (AM2-111) and after (AM2-122) hydrolysis, have been characterized by XRD, XPS and TEM analysis.[14]

XRD studies have shown that metallic crystalline phases are already present in the samples obtained by contacting the oxide matrix with the toluene solution of the platinum precursor (see Fig. 1). They are presumably formed by contacting water, coming from the condensation of surface silanols or fortuitously encountered in the course of the sample preparation. The broad peak centred at $2\theta \approx 39.7°$ was indexed as the (111) reflection of the *fcc* structure of metallic platinum (JCPDS Card No. 4-802,2000). Treatment with water vapour at 40 °C promoted further crystallization, as evidenced by the moderate sharpening of the (111) peak and the slight intensity increase of the weak (200) platinum reflection ($2\theta \approx 46°$). The average crystallite size was estimated, by using the Scherrer equation, to be ≈ 6 nm for both samples, although it can be over-estimated, as only the larger particles contribute to the diffraction.

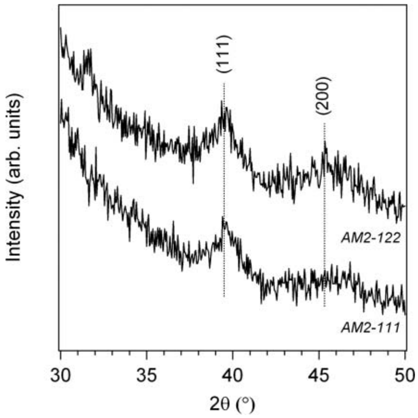

Fig. 1 XRD patterns of Pt-loaded silica samples before (AM2-111) and after (AM2-122) exposure to water vapour.

Further information on the chemical composition of both samples was obtained by XPS analysis: the platinum content was about 0.08 at.%, in agreement with the value of 0.76 wt% obtained by ICP measurements (see Experimental section). In Fig. 2, the XPS high resolution spectra of the Pt4*f* regions for samples A (AM2-111) and B (AM2-122) clearly show the $4f_{7/2}$ and $4f_{5/2}$ spin–orbit splitting components. Both spectra show a significant line broadening suggesting the presence of platinum centres characterized by different oxidation states and/or chemical environments. Peak deconvolution resulted in two doublets centred at (BE $Pt_{4f7/2}$) ≈71.5 eV and ≈73.0 eV, assigned to Pt(0) and Pt(II) species, respectively.[15] The most remarkable difference between the samples concerns the amount of metallic platinum, that can be evaluated by comparing the intensity of the Pt(0) and Pt(II) components.

While the Pt(0)/Pt(II) ratio is *ca.* 1 in the as-prepared Pt-SiO_2 sample (A), it increases to *ca.* 2.2 after hydrolysis. Therefore, contacting the toluene solution of $Pt_2(\mu\text{-}Cl)_2Cl_2(CO)_2$ with the

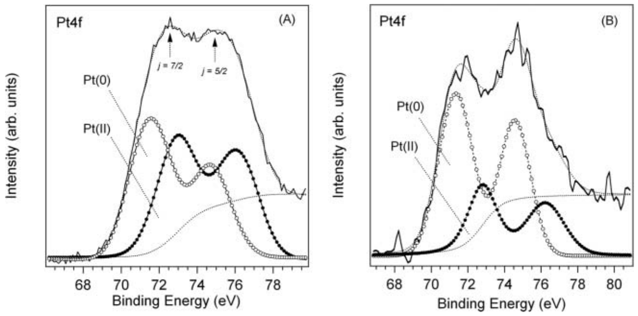

Fig. 2 Pt4*f* XPS spectra of the Pt-loaded silica samples before (A, AM2-111) and after (B, AM2-122) exposure to water vapour.

silica matrix produces a reduction of about half of the Pt(II) ions, whereas further Pt(II) → Pt(0) reduction is achieved through water vapour treatment, up to at least 70% of the total platinum content. In both samples, the presence of some Cl^- ions adsorbed on the silica surface was also observed. As a matter of fact, the position (≈199 eV) of the Cl2p line is typical for chloride species.

TEM analysis of the particle size distribution in a significant region of the samples showed that the particles in AM2-111 had a smaller diameter than in AM2-122. Fig. 3 shows images of the platinum crystallites in the two samples (A: AM2-111; B: AM2-122).

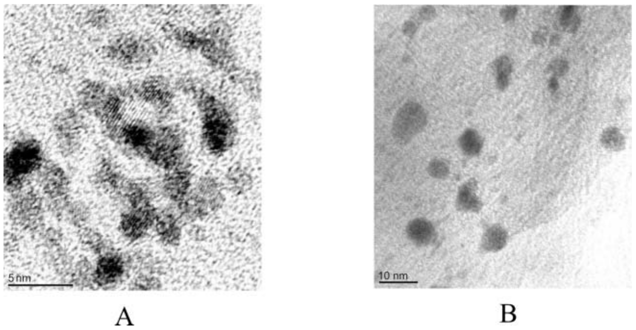

A

B

Fig. 3 TEM images of platinum aggregates on silica obtained by using $Pt_2(\mu\text{-}Cl)_2Cl_2(CO)_2$ as precursor. A: sample AM2-111; B: sample AM2-122.

In order to study the corresponding phenomenon with palladium, the same silica support was contacted with an orange toluene solution of $Pd_2(\mu\text{-}Cl)_2Cl_2(CO)_2$. The process was carried out at room temperature under a CO atmosphere in order to contrast the spontaneous decarbonylation of the palladium complex before its contact with the support.[7b] The migration of the palladium-containing fragments from the yellow solution to the SiO_2 surface was evidenced by the colour transfer from the solution to the support. As in the case of the platinum loading, this step was followed by treatment at 40 °C in the presence of water vapour. Also the palladium-loaded silica samples, before (AM3-66) and after (AM3-69) hydrolysis, have been characterized by XPS, XRD and TEM analysis.

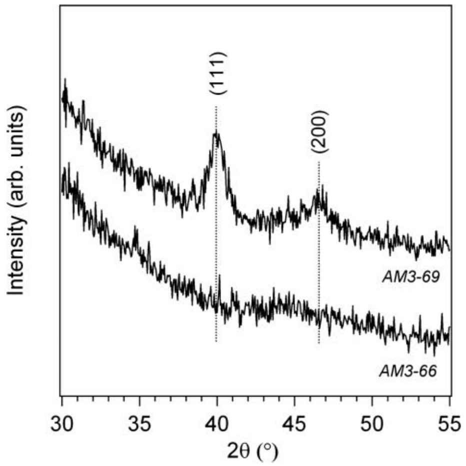

Fig. 4 XRD analysis of Pd-SiO_2 samples before (AM3-66) and after (AM3-69) exposure to moisture.

Concerning the sample microstructure, from the XRD diffraction patterns reported in Fig. 4 it can be clearly observed that crystallization depends on sample treatment. As a matter of fact, an amorphous pattern without any detectable crystalline phase is observed for the Pd-SiO_2 obtained by contacting the silica matrix with the toluene solution of $Pd_2(\mu\text{-}Cl)_2Cl_2(CO)_2$. After exposure to moisture, the appearance of two diffraction peaks indicates a remarkable variation of the sample microstructure. The peaks centred at $2\theta \approx 40.1°$ and $2\theta \approx 46.6°$ are indexed as the (111) and (200) reflexes of the *fcc* structure of metallic palladium (JCPDS Card No. 46-1043, 2000). The mean diameter of the Pd nanocrystallites, as evaluated using the Scherrer equation, is *ca.* 6 nm: as already anticipated, we expect that only the largest particles contribute to the diffraction.

XPS investigation evidenced that metallic palladium is already present in the as-prepared sample. Fig. 5 shows the XPS high resolution spectra of the Pd3*d* regions, with the $d_{5/2}$ and $d_{3/2}$ spin–orbit splitting components, for the as-prepared Pd-SiO_2 (A, AM3-66) and after hydrolysis (B, AM3-69). A moderately broad band-shape profile can be observed especially for the as-prepared sample, suggesting the presence of palladium centres with different oxidation states and/or chemical surroundings. The changes between sample A and sample B in the Pd3*d* spectra became more apparent by fitting two doublet components to the data. In both cases, the positions of the components at (BE Pd3$d_{5/2}$) ≈335.2 eV and ≈337.0 eV, corresponding to Pd(0) and Pd(II) species, respectively.[15] It is worth highlighting that, by comparing the intensities of the Pd(0) and Pd(II) components, metallic palladium represents *ca.* 65% of the total metal content in the as-prepared Pt–SiO_2 sample (A) increasing up to 85% after hydrolysis. Therefore, contacting the toluene solution of the $Pd_2(\mu\text{-}Cl)_2Cl_2(CO)_2$ compound with the silica matrix is effective in promoting the Pd(II)-to-Pt(0) conversion, which is

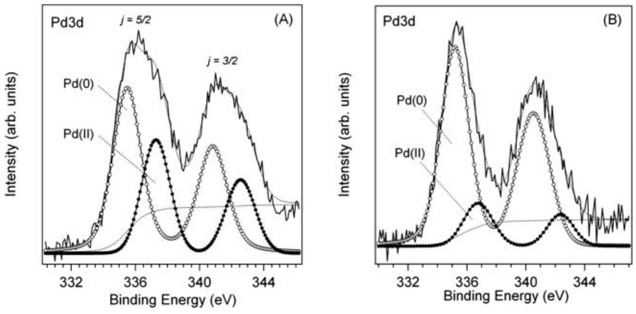

Fig. 5 Pd3*d* XPS spectra of the Pd-loaded silica samples before (AM3-66, A) and after (AM3-69, B) exposure to water vapour.

almost complete after controlled exposure to moisture under mild conditions. XPS analysis reveals a palladium content of 0.12 at.% in the as-prepared sample (in agreement with the ICP elemental analysis, see Experimental section), which apparently decreases to ~ 0.06 at.% after treatment with moisture: a possible explanation is the aggregation of Pd atoms to larger particles which are not completely detected by XPS. The Cl2p region was observed in the as-prepared Pd–SiO_2 (A, AM3-66) sample, centred at a position typical for chloride species (≈199 eV), thus suggesting that some Cl^- ions remained adsorbed on the silica surface. After hydrolysis (B, AM3-69), the chloride was practically undetected.

TEM analysis of the particle size distribution in a significant region of the sample AM3-66 showed that the particles had a smaller diameter than in AM3-69 (see Fig. 6).

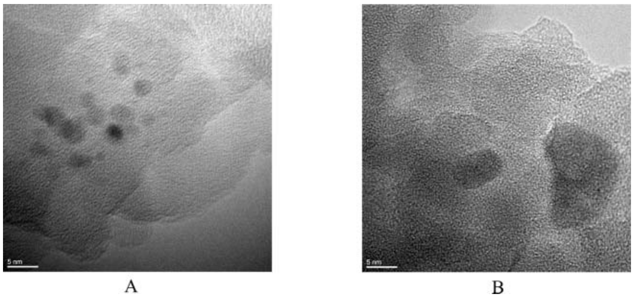

Fig. 6 TEM images of the palladium aggregates (A: AM3-66; B: AM3-69).

Catalytic hydrogenations

The catalytic activity of these materials has been evaluated in the hydrogenation of cyclohexene, carried out at room temperature and at atmospheric pressure in cyclohexane as solvent. The reactions, which were monitored by measuring the hydrogen uptake, are independent of the olefin concentration. A sequence of experiments was performed by adding fresh alkene when the hydrogenation was complete, showing that the catalytic activity was maintained and even enhanced. The catalytic performance expressed as the H_2/M molar ratio per hour, M being the total metal content, corresponds to 890 h^{-1} and 340 h^{-1} for the platinum- and the palladium-loaded silica, respectively. Plots reporting the [absorbed H_2]/metal molar ratio *vs.* time are shown in Fig. 7 and 8 of the Experimental section.

In Table 1 these data are compared with some literature information for the same reaction carried out with palladium- or platinum-based catalysts under similar conditions.

It appears that the catalytic efficiency is only moderately affected by the nature of the molecular precursor. For instance, the presence of CO, Cl or Br in the precursor does not compromise the activity of the final catalyst. Nevertheless, it is interesting to note that in the experiments reported in the present paper (items 1 and 5 of Table 1) the pre-treatment of the catalyst is limited to its exposure to water vapour at 40 °C (see Experimental), while in other cases a pre-treatment at higher temperature (200–250 °C) is necessary to observe rate independence of the olefin concentration (for instance items 3 and 6).

Commercial catalysts perform similarly.

Experimental

General information and instrumentation

All operations were performed under an atmosphere of pre-purified dinitrogen, or carbon monoxide, as specified. Solvents were dried by conventional methods prior to use. The starting materials *cis*-$PtCl_2(CO)_2$, $Pt_2(\mu\text{-}Cl)_2Cl_2(CO)_2$ and $Pd_2(\mu\text{-}Cl)_2Cl_2(CO)_2$ were prepared according to the literature.[6,7] Commercial silica (Grace, EP 17G, surface area 325 m^2 g^{-1}, pore volume 1.82 cm^3 g^{-1}) was treated at 160 °C over P_4O_{10} for 12 h *in vacuo* up to a constant weight and then stored in flame-sealed vials under an atmosphere of dry N_2. On the basis of our past experience this type of

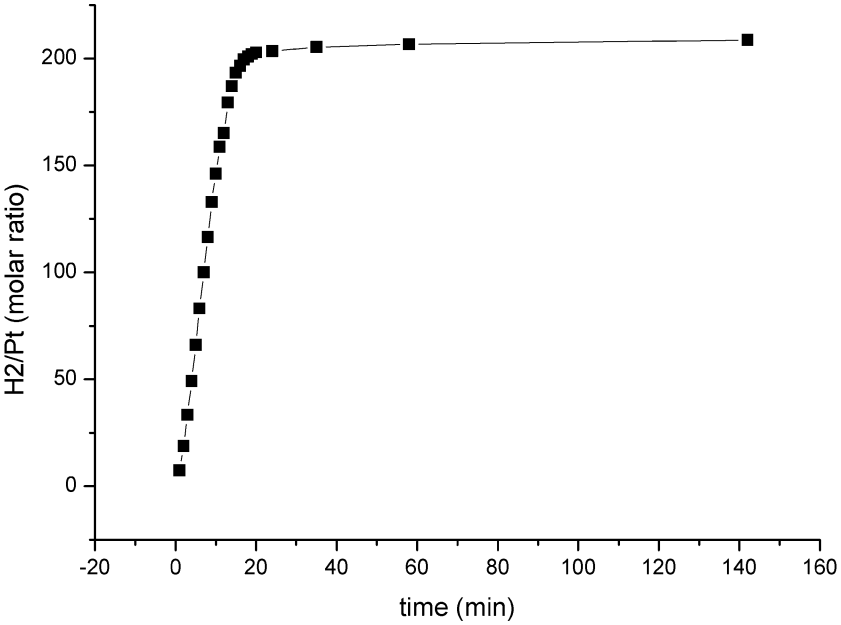

Fig. 7 Molar ratio (absorbed H_2)/Pt *vs.* time for the platinum-catalyzed reduction of cyclohexene. For the reaction conditions, see text.

Table 1 Efficiency of palladium- and platinum-based catalysts in cyclohexene hydrogenation[a]

	Metal	Precursor	T/°C	P/MPa	$[(H_2/M)]\ h^{-1}$	Ref.
1	Pt/SiO_2	$Pt_2(\mu\text{-}Cl)_2Cl_2(CO)_2$	24.9	0.1	890	This work
2	Pt/SiO_2	$PtCl_2(CO)_2$	20	0.1	720	5a
3	Pt/SiO_2	$Pt(O_2CNEt_2)_2L_2$	20	0.1	340	4a
4	PtO_2[b]		75	0.4	250	16
5	Pd/SiO_2	$Pd_2(\mu\text{-}Cl)_2Cl_2(CO)_2$	24.9	0.1	340	This work
6	Pd/SiO_2	$Pd(O_2CNEt_2)_2(NHEt_2)_2$	24	0.1	400	4b
7	Pd/pol	$PdCp(C_3H_5)$	25	0.2	300	17
8	Pd colloid	$[NR_4]_2[PdCl_2Br_2]$	20	0.1	217	18
9	Pd/C 1%[c]		30	0.1	200	19

[a] The column before the last one reports the experimentally observed H_2/M molar ratio *per* hour. In experiments 1 and 5, described in this paper, no pre-treatment of the catalyst was carried out. The Pt- and Pd-loaded silica samples of experiments 2, 3 and 6 had been treated at 210–230 °C before use. The Pd(0) coordination polymer (Pd/pol) used in experiment 7 was prepared by reacting $PdCp(C_3H_5)$ with 4,4′-diisocyanobiphenyl and was pre-hydrogenated (15 h) before use. The Pd colloid of experiment 8 was prepared by reacting $PdCl_2$ with $N(C_8H_{17})_4Br$ in 1:2 molar ratio in refluxing THF and then treating the obtained solution with H_2 ($P = 1$ bar, room temperature) for 14 d. [b] Adams' catalyst. [c] Commercialized by Aldrich.

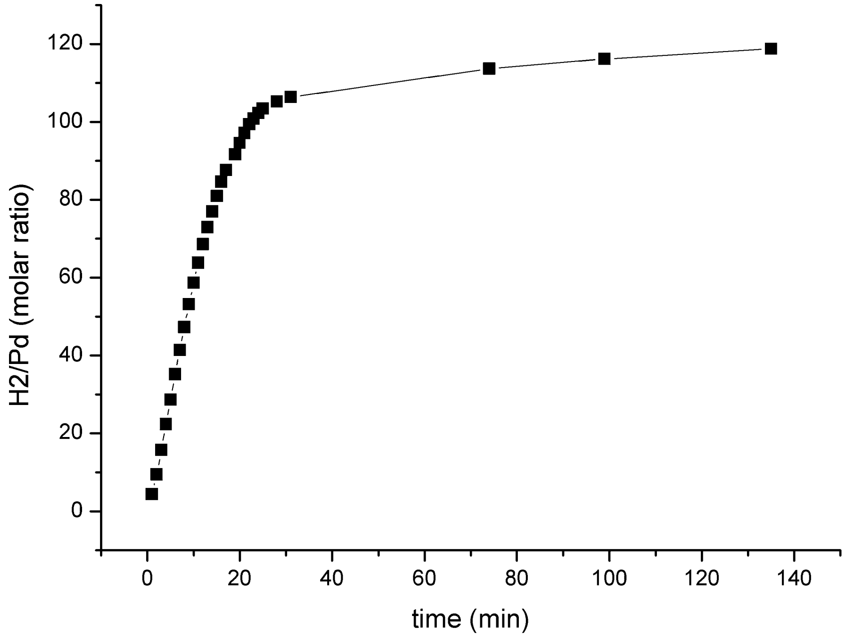

Fig. 8 Molar ratio (absorbed H_2)/Pd *vs.* time for the palladium-catalyzed reduction of cyclohexene. For the reaction conditions, see text.

pre-treatment eliminates most of the hydrogen-bonded water from the surface, leaving most of the hydroxyl groups ≡Si–OH, which are chemically reactive towards the metal precursor. The total silanol content (typically, between 2.8 and 3.1 mmol g^{-1} corresponding to 6 OH groups per square nanometer) was estimated from the mass loss upon further heating at 850 °C.

Elemental analyses (C, H, N) were performed at Dipartimento di Scienze Farmaceutiche, Università di Pisa, with a C. Erba mod. 1106 elemental analyzer. Pt, Pd and Cl elemental analyses on the molecular precursors were carried out by reduction of the products with sodium formate: metal black was filtered off, dried and weighed. The Volhard method was applied to the filtrate. Pd and Pt content in the metal-loaded silica was obtained by ICP-AES with a Perkin-Elmer Plasma II instrument. The gas-volumetric measurements were carried out according to the method described by Calderazzo and Cotton.[20]

IR spectra were recorded with a mod. 1725X FT-IR Perkin-Elmer spectrophotometer in solution or as Nujol or polychlorotrifluoroethylene (PCTFE) mulls, as specified in each case, prepared under exclusion of moisture. Diffuse Reflectance Infrared Fourier Transform (DRIFT) spectra were measured with the same instrument by mixing the samples with dry KBr under an inert atmosphere and by rapid transfer to the cell (Spectra Tech).

The composition of the samples was investigated by XPS. The analyses were performed with a Perkin-Elmer Φ 5600-ci spectrometer using non-monochromatized Mg-K_α radiation (1253.6 eV). The working pressure was $\leq 5 \times 10^{-8}$ Pa. The spectrometer was calibrated by assuming the binding energy (BE) of the Au $4f_{7/2}$ line at 83.9 eV with respect to the Fermi level. The standard deviation for the BE values was 0.15 eV. The reported BE's were corrected for the charging effects, assigning a value of 284.8 eV to the C1s line of adventitious carbon.[21] Survey scans were obtained in the 0–1200 eV range. Detailed scans were recorded for the C1s, N1s, O1*s*, Cl2*p*, Si2*p*, Pd3*d* and Pt4*f* regions. The analysis involved Shirley-type background subtraction,[22] non-linear least-squares curve fitting, adopting Gaussian–Lorentzian peak shapes and peak area determination by integration. The atomic compositions were evaluated from peak areas using sensitivity factors supplied by Perkin-Elmer, taking into account the geometric configuration of the apparatus. The uncertainty on atomic composition values is *ca.* 5–10%. The powders were pressed into pellets and introduced into the XPS analytical chamber through a fast entry lock system.

XRD measurements have been performed using a Philips PW 1820 diffractometer (Cu-K_α radiation, 40 kV, 50 mA) equipped with a thin film attachment (glancing angle = 0.5°). Selected angular ranges were step-scanned several times up to a satisfactory signal-to-noise ratio. For the microstructure characterization, an improved profile fitting method using a pseudo-Voigt representation for the line profiles was used. The average crystallite size was calculated using the Scherrer equation, taking into account the instrumental broadening.

TEM measurements were carried out with a Jeol JEM 2010 instrument operating at 200 kV. A small amount of specimen was ground in a mortar to a very fine powder, which was deposited on a lacy carbon film supported on a standard copper grid. The whole sequence of operations was carried out under a dry N_2 atmosphere. The time required for sample preparation was minimized in order to avoid deterioration or contamination.

Reaction of *cis*-$PtCl_2(CO)_2$ with H_2O in toluene

Under N_2 atmosphere. A solution of *cis*-$PtCl_2(CO)_2$ (2.68 g, 8.3 mmol) in toluene (50 mL) was treated with a solution of water (150 μL, 8.3 mmol) in toluene (400 mL). The toluene solution of water was added dropwise to the solution containing the platinum precursor. After 1 h stirring an IR spectrum of the solution showed the presence of a consistent amount of unreacted *cis*-$PtCl_2(CO)_2$. Subsequent direct additions (75 μL each, 4.15 mmol) of H_2O were performed with a micro-syringe up to a final H_2O/Pt molar ratio of 3, under IR monitoring. At every addition, the amount of the black solid was observed to increase and simultaneously the concentration of *cis*-$PtCl_2(CO)_2$ in the liquid phase decreased (IR), up to complete disappearance of the typical carbonyl stretching bands at 2168 and 2127 cm $^{-1}$. After further stirring at 50 °C for 30 min, the suspension was filtered and the solid was dried *in vacuo* (1.23 g, 57% yield based on the platinum content). Anal. Calcd (%) for $[PtCl(CO)]_n$: Pt, 75.4; Cl, 13.7. Found: Pt, 77.1; Cl, 11.8. IR (Nujol): ν_{CO}, 2060 cm^{-1}. The black solid thus obtained was subjected to the following experiments.

(a) The product (280 mg, 1.1 mmol of Pt) was introduced under a N_2 atmosphere into a Schlenk tube containing CH_2Cl_2 (25 mL) and $[NBu_4]Cl$ (313 mg, 1.1 mmol) was added to the resulting suspension. After 12 h, IR bands attributable to $[NBu_4]_2[Pt_2Cl_4(CO)_2]$ were observed at 2048 and 2028 cm^{-1}. The suspension was filtered, and the filtrate was evaporated to dryness under reduced pressure. The solid residue of $[NBu_4]_2[Pt_2Cl_4(CO)_2]$ was dried *in vacuo* (424 mg, 72% yield). Anal. Calcd (%) for $[NBu_4]_2[Pt_2Cl_4(CO)_2]$, $C_{34}H_{72}Cl_4N_2Pt_2$: C, 38.1; H, 6.8; N, 2.6. Found: C, 37.9; H, 6.7; N, 2.7. IR (Nujol): ν_{CO}, 2043 and 2022 cm^{-1}.

(b) Under N_2 atmosphere, the product $[PtCl(CO)]_n$ was reacted with an excess of water in toluene; HCl was evolved and the formation of platinum metal (95% yield) was established.

Under CO atmosphere. To a solution of *cis*-$PtCl_2(CO)_2$ (290 mg, 0.90 mmol) in toluene (35 mL), additions (8 μL each, 0.45 mmol) of H_2O were performed with a micro-syringe up to a H_2O/Pt molar ratio of 2.5, when the platinum chloro-carbonyl had disappeared (IR) from the solution. Each addition of water was accompanied by an almost immediate precipitation of a solid. The violet precipitate of $[Pt(CO)_2]_n$, after drying in a CO stream (221 mg, 97% yield), showed IR (Nujol) bands at 2071 and 1889 cm^{-1}.

In another experiment carried out under CO, preformed $[PtCl(CO)]_n$ (0.228 mg, 0.88 mmol of platinum), prepared as described above, was suspended in 50 mL of toluene and 2.7 mmol of water was added. The initially black solid became violet in about 15 min: after some hours stirring the violet solid, $[Pt(CO)_2]_n$, was filtered, briefly dried in a CO stream and sealed in vials under CO (90% yield).

Loading silica with metals

Platinum. In a typical experiment, a solution of $Pt_2(\mu\text{-}Cl)_2Cl_2(CO)_2$ (0.25 g, 0.85 mmol of platinum, ν_{CO} = 2130 cm^{-1}) in toluene (150 mL) was added to pre-treated silica (7.9 g corresponding to 25.5 mmol of silica-bonded hydroxyl groups, ≡SiOH). A prompt colour fading of the solution was observed, and, after 15 h stirring, an IR spectrum of the liquid phase showed the band of the unconverted material at 2130 cm^{-1} to be definitely of lower intensity than initially. The suspension was filtered and the pale-yellow solid was dried *in vacuo*, finally yielding the dry pale-yellow substance (AM2-111, 7.67 g). Anal. (%): C, 0.49; H, 0.18; Pt, 0.76. DRIFT: 2116 cm^{-1}. The XRD and XPS spectra are in Fig. 1 and 2, respectively. For TEM data, see Fig. 3A: the particle diameters range from 0.3 to 2.6 nm.

A portion of the platinum-loaded silica (1.26 g) was exposed at 40 °C for 8 h to water vapour originated from an aqueous solution of NaOH (2.5%). The silica became gradually grey. After drying *in vacuo* in the presence of P_4O_{10}, no DRIFT bands attributable to platinum-bonded carbonyl groups were observed. The final substance was classified as AM2-122. TEM data, see Fig. 3B, showed particle diameters ranging from 0.5 nm to 6.8 nm.

Samples of silica thus obtained were used for the catalytic hydrogenation experiments.

Palladium. Under an atmosphere of carbon monoxide, an orange solution of 0.181 g of $Pd_2Cl_4(CO)_2$ in 50 mL of toluene (0.88 mmol of palladium, ν_{CO} = 2161 cm^{-1}) was added to a suspension of 9.1 g of silica in 100 mL of toluene. Within 24 h stirring at room temperature, the liquid phase of the mixture became colourless and the resulting yellow solid was recovered by filtration, dried *in vacuo* and sealed under dinitrogen (AM3-66, 7.35 g). Anal. (%): C, 0.48; H, 0.23; Pd, 0.76. DRIFT: 1978 cm^{-1}. The XRD and XPS spectra are in Fig. 4 and 5A, respectively. For TEM data see Fig. 6A.

A portion of the solid, maintained at 40 °C, was contacted for 8 h with water vapour generated from a 2.7% solution of NaOH. After drying *in vacuo* at room temperature, the reflectance spectra of the solid showed no bands attributable to palladium-bonded carbonyl groups. The resulting grey-coloured silica (AM3-69) was sealed under dinitrogen in glass vials. TEM data, see Fig. 6B, showed particle diameters ranging from 2.4 to 6.1 nm.

Samples of silica thus obtained were used for the catalytic hydrogenation experiments.

Catalytic hydrogenation of cyclohexene

Platinum-catalyzed hydrogenation. A reactor containing 25 mL of cyclohexane saturated with dihydrogen and a flame-sealed thin-walled glass ampoule containing the platinum-loaded silica (0.143 g, 5.6 × 10^{-3} mmol of platinum) was connected to a gas-volumetric apparatus under a dihydrogen atmosphere. By operating at 24.9 °C, 0.7 mL of a 1.69 M solution of cyclohexene in cyclohexane were introduced (1.18 mmol, corresponding to a cyclohexene/Pt molar ratio of 211). When the ampoule was broken, the absorption of H_2 started. It was recorded as a function of time and found to be substantially linear, corresponding to 14.8 (mmol of H_2) × min^{-1} × $mmol_{Pt}^{-1}$. The plot of the molar ratio (absorbed H_2)/Pt *vs.* time of a typical experiment is in Fig. 7.

Palladium-catalyzed hydrogenation. A reactor containing 20 mL of cyclohexane saturated with dihydrogen and a flame-sealed thin-walled glass ampoule containing the palladium-loaded silica (0.134 g, 9.6 × 10^{-3} mmol of metal) was connected with a gas-volumetric apparatus under a dihydrogen atmosphere. By operating at 24.9 °C, 0.7 mL of a solution of cyclohexene in cyclohexane (1.69 M, 1.18 mmol) were introduced, corresponding to a cyclohexene/Pd molar ratio of 123. After breakage of the ampoule, the absorption of H_2 *vs.* time was measured and found to be substantially linear and corresponding to 5.6 (mmol of H_2) × min^{-1} × $mmol_{Pd}^{-1}$. The plot of the molar ratio (absorbed H_2)/Pd *vs.* time is in Fig. 8.

Conclusion

Our approach to the preparation of the palladium- or platinum-containing catalysts was based on an attempt to minimize the intrinsic differences between the two metals in the process of loading on the inorganic matrix. As the metal particles were prepared by a substantially identical process at room temperature, starting from molecular precursors of the same type, we are confident that our goal was accomplished, although we cannot avoid differences induced by the different nature of the metal atoms; particularly important is the different mass and the different momentum which may affect the migration phenomenon on the surface of the support. Previous suggestions have been made[23] that palladium should possess a catalytic activity similar to, or even higher than, that of platinum in hydrogenation reactions. However, earlier papers[24] have reported conflicting evidence about this point. It is important to point out that both platinum and palladium crystallize in the *fcc* structure and that the corresponding atomic radii (for CN = 12) have similar values (Å): platinum, 1.39; palladium, 1.37.[25] Thus, metal particles of the same dimensions should contain the same number of atoms and the same percentage of exposed atoms. In our case the average diameters of the metal particles in the platinum- and palladium-loaded silica used in the catalytic tests are 1.6 and 4.5 nm, respectively. It follows that the percentage of exposed metal atoms should be about 60 and 30% in the platinum and palladium samples, respectively. Thus, the apparent lower activity of palladium can be attributed to a morphological aspect rather than to an intrinsic property. We can therefore confirm the conclusions by Boudart[23] that the catalytic activity of the two metals is similar.

Acknowledgements

This work was financially supported by the research projects CNR-INSTM PROMO, FIRB-MIUR RBNE033KMA "Molecular compounds and hybrid nanostructured materials with resonant and non-resonant optical properties for photonic devices", FISR-MIUR "Inorganic hybrid nanosystems for the development and the innovation of fuel cells", CARIPARO 2006 "Multi-layer optical devices based on inorganic and hybrid materials by innovative synthetic strategies" and by *Ministero dell'Università e della Ricerca Universitaria* (MIUR), 2004–6. Thanks are due to: Chimet, S.pA., Badia al Pino, Arezzo, Italy, for loans of platinum and palladium, and for the analyses of the metal content in most of the silica-supported systems; Prof. E. Tondello, Università di Padova, for his interest and encouragement; Prof. P. Colombo and Prof. A. Martucci, Università di Padova, for XRD measurements and helpful discussions.

References

1 (*a*) P. K. Jain, X. Huang, I. H. El-Sayed and E. M. El-Sayed, *Acc. Chem. Res.*, 2008, **41**, 1578; (*b*) I. Favier, S. Massou, E. Teuma, K. Philippot, B. Chaudret and M. Gómez, *Chem. Commun.*, 2008, 3296; (*c*) G. A. Samorjai, F. Tao and J. Y. Park, *Top. Catal.*, 2008, **47**, 1; (*d*) R. W. Murray, *Chem. Rev.*, 2008, **108**, 2688; (*e*) D. Astruc, Transition-metal Nanoparticles in Catalysis: From Historical Background to the State-of-the Art in *Nanoparticles and Catalysis,*ed. D. Astruc, Wiley-VCH Verlag, Weinheim, 2008, pp. 1–48; (*f*) H. Bönnemann and K. S. Nagabhushana, Metal Nanoclusters: synthesis and strategies for their size control in *Metal Nanoclusters in Catalysis and Materials Science, The Issue of Size Control*, ed. B. Corain, G. Schmid and N. Toshima, Elsevier B. V., Amsterdam, 2008, pp. 21–48.
2 D Poondi and M. A. Vannice, *J. Catal.*, 1996, **161**, 742.
3 For palladium–catalyzed hydrogenations, see: (*a*) Y. Gao, C.-A. Chen, H.-M. Gau, J. A. Bailey, E. Akhadov, D. Williams and H.-L. Wang, *Chem. Mater.*, 2008, **20**, 2839; (*b*) A. M. Doyle, S. K. Shaikhutdinov and H.-J. Freund, *Angew. Chem., Int. Ed.*, 2005, **44**, 629; (*c*) For platinum-catalyzed hydrogenations, see: F. O. Ernst, R. Büchel, R. Strobel and S. E. Pratsinis, *Chem. Mater.*, 2008, **20**, 2117; (*d*) T. Onoe, S. Iwamoto and M. Inoue, *Catal. Commun.*, 2007, **8**, 701.
4 (*a*) L. Abis, D. Belli Dell'Amico, C. Busetto, F. Calderazzo, R. Caminiti, C. Ciofi, F. Garbassi and G. Masciarelli, *J. Mater. Chem.*, 1998, **8**, 751; (*b*) L. Abis, D. Belli Dell'Amico, C. Busetto, F. Calderazzo, R. Caminiti, F. Garbassi and A. Tomei, *J. Mater. Chem.*, 1998, **8**, 2855; (*c*) L. Abis, L. Armelao, D. Belli Dell'Amico, F. Calderazzo, F. Garbassi, A. Merigo and E. A. Quadrelli, *J. Chem. Soc., Dalton Trans.*, 2001, 2704.
5 (*a*) D. Belli Dell'Amico, F. Calderazzo, C. Ciofi, F. Garbassi, L. Grande and G. Masciarelli, *J. Cluster Sci.*, 1998, **9**, 473; (*b*) A. Merigo, *Ph.D. Thesis*, University of Pisa, 2000.
6 (*a*) B. P. Andreini, D. Belli Dell'Amico, F. Calderazzo and M. G. Venturi, *J. Organometal. Chem.*, 1988, **354**, 357, and references therein; (*b*) F. Bagnoli, D. Belli Dell'Amico, F. Calderazzo, U. Englert, F. Marchetti, A. Merigo and S. Ramello, *J. Organomet. Chem.*, 2001, **622**, 180, and references therein.
7 (*a*) D. Belli Dell'Amico and F. Calderazzo, *Inorg. Chem.*, 1981, **20**, 1310; (*b*) D. Belli Dell' Amico, F. Calderazzo and N. Zandonà, *Inorg. Chem.*, 1984, **23**, 137.
8 *CRC Handbook of Chemistry and Physics*, 82nd edn, ed. D. R. Lide, Boca Raton, 2001–2, pp. 9–63.
9 S. Ramello, *Chemistry Degree Thesis*, University of Pisa, 1996.
10 I. V. Fedoseev and A. S. Gordeev, *Zh. Neorg. Khim.*, 2007, **52**, 12; I. V. Fedoseev and A. S. Gordeev, *Chem. Abstr.*, 2007, **148**, 134337.
11 (*a*) G. Booth, J. Chatt and P. Chini, *Chem. Commun.*, 1965, 639; (*b*) G. Booth and J. Chatt, *J. Chem. Soc. A*, 1969, 2131.
12 (*a*) P. L. Goggin and R. J. Goodfellow, *J. Chem. Soc., Dalton Trans.*, 1973, 2355; (*b*) A. Modinos and P. Woodward, *J. Chem. Soc., Dalton Trans.*, 1975, 1516.

13 D. Belli Dell'Amico, F. Calderazzo, M. Dittmann, L. Labella, F. Marchetti, E. Schweda and J. Strähle, *J. Organomet. Chem.*, 1999, **583**, 162, and references therein.
14 *Applications of Physical Methods to Inorganic and Bioinorganic Chemistry*, ed. R. A. Scott and C. M. Lukehart, J. Wiley, Chichester, West Sussex, 2007.
15 J. M. Moulder, W. F. Stickle, P. E. Sobol and K. D. Bomben, *Handbook of X-ray Photoelectron Spectroscopy*, Perkin-Elmer Corporation, Eden Prairie, MN, 1992 [http:www.//srdata.nist.gov/xps/].
16 C. W. Scheeren, G. Machado, J. Dupont, P. F. P. Fichtner and S. R. Texeira, *Inorg. Chem.*, 2003, **42**, 4738.
17 I. Feinstein-Jaffe and A. Efraty, *J. Mol. Catal.*, 1986, **35**, 285.
18 H. Bönnemann, R. Brinkmann, R. Köppler, P. Neiteler and J. Richter, *Adv. Mater.*, 1992, **4**, 804.
19 M. V. Seregina, L. M. Bronstein, O. A. Platonova, D. M. Chernyshov, P. M. Valetsky, J. Hartmann, E. Wenz and M. Antonietti, *Chem. Mater.*, 1997, **9**, 923.
20 F Calderazzo and F. A. Cotton, *Inorg. Chem.*, 1962, **1**, 30.
21 D. Briggs and M. P. Seah, *Practical Surface Analysis*, J. Wiley, Chichester, Vol. 1, 1990.
22 D. A. Shirley, *Phys. Rev. B*, 1972, **5**, 4709.
23 (*a*) M. Boudart and D. J. Sajkowski, *Faraday Discuss.*, 1991, **92**, 57; (*b*) M. Boudart, *Chem. Rev.*, 1995, **95**, 661.
24 (*a*) E. Segal, R. J. Madon and M. Boudart, *J. Catal.*, 1978, **52**, 45; (*b*) E. E. Gonzo and M. Boudart, *J. Catal.*, 1978, **52**, 462.
25 A. F. Wells, *Structural Inorganic Chemistry*, 5th edn, Clarendon Press, Oxford, 1984, p. 1288.